Nano Energy 76 (2020) 105052

Contents lists available at ScienceDirect

Nano Energy

journal homepage: http://www.elsevier.com/locate/nanoen

A novel hybridized blue energy harvester aiming at all-weather IoT applications

Long Liu [a,b,c,d], Qiongfeng Shi [a,b,c,d], Chengkuo Lee [a,b,c,d,e,*]

[a] Department of Electrical and Computer Engineering, National University of Singapore, 4 Engineering Drive 3, Singapore, 117576, Singapore
[b] Center for Intelligent Sensors and MEMS, National University of Singapore, Block E6 #05-11, 5 Engineering Drive 1, Singapore, 117608, Singapore
[c] Hybrid-Integrated Flexible (Stretchable) Electronic Systems Program (HIFES), National University of Singapore, Block E6 #05-3, 5 Engineering Drive 1, Singapore, 117608, Singapore
[d] NUS Suzhou Research Institute (NUSRI), Suzhou Industrial Park, Suzhou, 215123, PR China
[e] NUS Graduate School for Integrative Science and Engineering (NGS), National University of Singapore, Singapore, 117456, Singapore

ARTICLE INFO

Keywords:
Triboelectric nanogenerator
Blue energy harvester
Hybridized energy harvester
Internet of Things
Low frequency vibration

ABSTRACT

A hybridized blue energy harvester based on triboelectric-electromagnetic hybridized generator is developed to extract the abundant energy from water waves. Within the pendulum design of the blue energy harvester, an interdigital electrodes based triboelectric nanogenerator (I-TENG), a switches based triboelectric nanogenerator (S-TENG) and an electromagnetic generator (EMG) are complementarily integrated, to more effectively scavenge the water wave energy after packaged in a waterproof enclosed box. The outputs of both TENGs are enhanced by an optimized flexible circular ring supporting a rolling magnet due to soft contact and induced larger contact area. With a novel designed hybridized circuit, output power can reach to 95.4 mW at load of 100Ω. After the management circuit, a lithium battery of 200 mAh can be charged from 3.07 V to 3.35 V by this blue energy harvester with six hours of water wave impaction. Besides using the hybridized blue energy harvester to power a digital temperature sensor directly and continuously, an all-weather IoT platform is also established with the blue energy harvester, a solar cell panel and a Bluetooth sensor module. The ambient information of humidity and temperature can be detected and sent to user-end by the Bluetooth sensor module under various conditions with or without daylight and water waves.

1. Introduction

Energy crisis is progressively becoming a challenged global problem, alongside increasing of worldwide energy demands and aggravation of environmental concerns [1,2]. Accordingly, utilization of renewable clean energy resources shows superiorities as an economic pathway to cope with above issues [3]. The ocean covering over 70% of the Earth's surface, contains abundant energy, and shows advantage of less dependence on weather, seasonality, and day-night rhythm [4]. The energy in ocean area referred to the blue energy, mainly in forms of water wave energy, tidal energy, ocean current energy, thermal energy, and osmotic energy, is one of the most promising renewable clean energy resources for large scaled practical applications [5]. Traditional blue energy harvesters are mostly based on the electromagnetic generator (EMG) and need extra complex mechanical and hydraulics structures converting wavy motions into linear reciprocal motion or rotary motion to drive the generators generating electricity [6,7]. However, the complicated structure and high cost limit them to be widely applied as blue energy harvesters [8].

Recently, the emergence of triboelectric nanogenerator (TENG) has brought a new route for harvesting blue energy of low frequency [8–14]. The TENG's origin can be derived to Maxwell's displacement current, and its operating mechanism is based on the conjugation of triboelectric effect and electrostatic induction [15–22]. This new technology has been considered as one of the most effective ways to harvest ambient mechanical energy with merits of high efficiency, high power density, low fabrication cost and environment friendly [23–27]. The TENG can effectively extract energy in the frequency range of <5 Hz due to its distinct mechanism, which is ideally suited for human motions [28–36] and water waves [37–45]. However, the devices applied in ocean area

* Corresponding author. Department of Electrical and Computer Engineering, National University of Singapore, 4 Engineering Drive 3, Singapore, 117576, Singapore.
E-mail address: elelc@nus.edu.sg (C. Lee).

https://doi.org/10.1016/j.nanoen.2020.105052
Received 7 May 2020; Received in revised form 28 May 2020; Accepted 3 June 2020
Available online 3 July 2020

need to cope with harsh climate and sustain pounding waves, which decrease outputs of the TENG by low surface charge density in humidity condition and inefficient charge transfer as varying wave motions [46–48]. Although lots of efforts in structure design [49–58], materials selection [59–65], and power management [66–69] are processed to improve the TENG's performance, current schemes for blue energy harvester are still inadequate.

To enhance the outputs of the blue energy harvester, multiple strategies of energy harvesting should be coupled to realize efficient cooperative work [70–75]. Prof. Ya Yang firstly invented the first electromagnetic-triboelectric hybridized nanogenerator in 2015, which can simultaneously scavenge mechanical energy from the same mechanical motions [76]. This method can largely enhance the conversion efficiency from mechanical energy to electricity, as compared with the individual electromagnetic generator or triboelectric nanogenerator [77–80]. Plentiful researches have proved that triboelectric-electromagnetic hybridized generator can effectively harvest mechanical energy original from human motion [81–85], objects' vibration [86,87], wind force [88–91] and water waves [92–95]. And different designs have applied to support synergetic operations of the TENG part and the EMG part, such as rotation axis, spring and linkage [93–100]. As for the blue energy harvester, a few kinds of waterproof packages are introduced to protect the core part away from water environment, such as spherical shell, box and cylinder tube [101–104]. However, the outputs still lag practical applications, especially for rapidly increased energy requirement of internet-of-things (IoT) devices ranging from industry electronics to personal electronics [105–109].

Herein, a hybridized blue energy harvester based on triboelectric-electromagnetic hybridized generator is developed to extract the abundant energy from water waves. Wherein an interdigital electrodes based triboelectric nanogenerator (I-TENG), a switches based triboelectric nanogenerator (S-TENG) and an electromagnetic generator (EMG) are complementarily integrated in a pendulum structure, and this pendulum can effectively scavenge water wave energy after packaged in a waterproof enclosed box. Benefit with the implied I-TENG, charges from the roller can also be utilized for energy harvesting. The outputs of both TENGs are enhanced by an optimized flexible circular ring supporting a rolling magnet due to soft contact and induced larger contact area. With a designed hybridized circuit using the integrated induction coil, whole output is further enhanced by combining three energy harvesting parts together. After the management circuit, a lithium battery of 200 mAh can be charged from 3.07 V to 3.35 V by this blue energy harvester with six hours of water wave impaction. Besides using the hybridized blue energy harvester to directly and continuously power a digital temperature sensor, an all-weather IoT platform is also established with the blue energy harvester, a solar cell panel and a Bluetooth sensor module. The ambient information of humidity and temperature can be detected and sent to user-end by the Bluetooth sensor module under various conditions with or without daylight and water waves. Moreover, the signals also can be sent and received eight times in 200 s under the situation of darkness benefit by the blue energy harvester operated in water waves, where the transmission rate is double of that only with solar cell operation, showing the great potential of the hybridized blue energy harvester for blue energy applications.

2. Results and discussion

Fig. 1 shows the schematic diagram of the hybridized blue energy harvester floating on the ocean surface, and details is illustrated in Fig. 1a. The inner side of the pendulum structure is revealed when taking the cover lid off. The I-TENG and the S-TENG are attached on the inner wall of the 3D printed body with a double-side VHB tape, and detailed operations are explained in experimental section. It is worth mentioning that the air gap is applied to maintain relative position between the magnet and the induction coil, and the centers are coincident when the pendulum structure is at the equilibrium position. A cylinder magnet with diameter of 30 mm is applied as the roller in the pendulum structure, with a length of 30 mm that is slightly shorter than the dimension of pendulum structure's parallel direction (35 mm). This magnetic roller can store potential energy and kinetic energy of the pendulum structure then release and roll by inertial effect. Thus, the I-TENG, the S-TENG and the EMG are driven to generate electricity when the magnet rolling

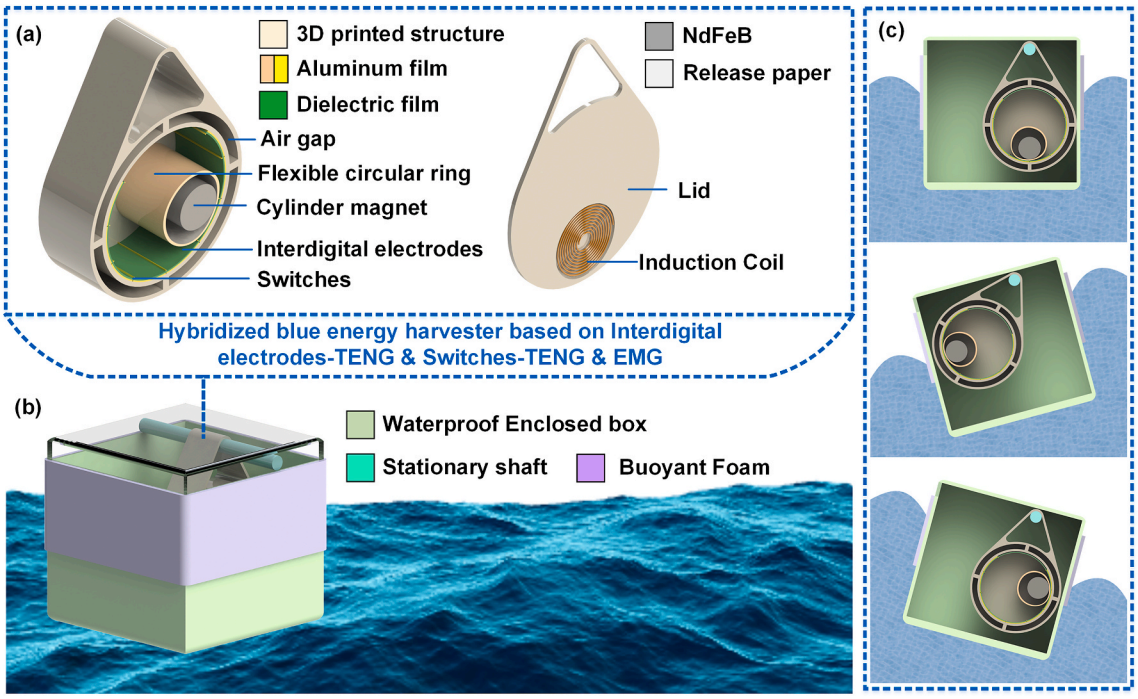

Fig. 1. (a) Schematic diagram of the pendulum structure containing an Interdigital electrodes-TENG (I-TENG), a Switches-TENG (S-TENG) and an Electromagnetic generator (EMG). (b) Schematic diagram of the hybridized blue energy harvester floating on ocean surface. (c) Working mechanism of the hybridized blue energy harvester under ocean wave at side view.

across relevant area. As shown in Fig. 1a, a paper-based flexible circular ring is set around the magnet, and conductive Aluminum film is attached on its outside surface. This lightweight deformable circular ring can roll with the magnet and contribute on enhancing the efficient contact area with TENGs' layers. As for EMG, the induction coil is placed on the lid and has a minimum distance of 3 mm away from the magnet. Such a device based on the triboelectric-electromagnetic hybridized generator is sealed for further testing.

Conceptual graph of the hybridized blue energy harvester is shown in Fig. 1b, where a waterproof enclosed box floating on water surface is applied to support the pendulum. A buoyancy foam circle of 25 mm thickness is attached on the box to avoid flip-over in varying waves. Along with the waves, the box can tilt and drive the pendulum structure swinging by the stationary shaft. The operation of this hybridized blue energy harvester is demonstrated in Fig. 1c. When the box is in horizontal position, the pendulum structure just state at the equilibrium position and hitinner wall of the box. Maximum swinging space is reserved for the pendulum structure, attributed to the position of the stationary shaft. When the box is tilting by the waves and the pendulum structure starts swinging to the empty space, the magnet and the flexible circular ring will roll to same direction. Through the swing, the pendulum can store extra potential and kinetic energy from waves. When the box recovers to the horizontal position, that swinging pendulum is stopped by the opposite wall while the inside magnet and the flexible circular ring keep rolling to the other direction. And the magnet and ring will continue rolling as the box is still tilting along with waves. Overall, the operations of this hybridized blue energy harvester are relied on box's status around waves, and the outputs are directly relative to inner parts of the pendulum structure.

To define and optimize the inner parts, effects of the flexible circular ring is discussed in Fig. 2. Beginning with the free-standing triboelectric nanogenerator, different sized of the circular rings are tested and compared with the raw magnet. As shown in Fig. 2a, the contact area between the circular ring and the pendulum structure is increasing with the increased diameter of rings. This trend is attributed to construction materials including the release paper and Aluminum tape. The circular ring with bigger diameter will be deformed more under gravity force, creating larger contact area. Corresponding outputs are presented in Fig. 2b and c, where the transferred charge quality and open circuit voltage are both increased as the increasing diameter of circular rings. Compared with the outputs of the raw magnet, the transferred charge quantity from 1# to 4# has increased by 30.7%, 94.8%, 254.7% and 535.8%, while the open circuit voltage from 1# to 4# has increased by 46.4%, 230%, 366.9% and 623.6%, respectively.

Next, the interdigital electrodes are introduced to take advantage of the efficient contact between the flexible circular ring and the pendulum structure, and this interdigital electrodes base triboelectric nanogenerator is named as I-TENG for short. As shown in Fig. 2d and e, the 3# ring is choosen to support the magnet due to its larger contact area compared to 1# and 2# ring, as well as the larger rolling space than the 4# ring. The inner wall of the pendulum structure is divided into six kinds of design illustrated in Fig. 2e, where the interdigital electrodes are evenly distributing on each side of the middle line at equilibrium position. Details exhibited in Fig. 2f show that number of charge transfer cycles is proportional to electrodes' number, which conform with mechanism of free-standing mode TENG. But with further increasing the electrodes's number to the VI-design, transferred charge quantity decreases significantly because of the adjacent interdigital electrode is completely coved by the deformed rolling ring and charge transferring between two interdigital electrodes is insufficient. When computing amount of transferred charge quantity in a cycle of rolling forward and back, the V-design obtain the maximum quantity as 401 nC, larger than the rest cases, where 207 nC in I-design, 228 nC in II-design, 229 nC in III-design, 294 nC IV-design and 246 nC in VI-design, illustrated in Fig. S1. Thus, the V-design of the interdigital electrodes is chosen for the I-TENG.

Furthermore, the S-TENG is introduced and discussed in Fig. 3. Aluminum strips are attached between two adjacent interdigital electrodes and used as switches to collect the charges on the magnet/rolling ring in Fig. 3a. Relevant working mechanism of I-TENG and the S-TENG are illustrated in Fig. 3b(i-x) with a raw magnet is applied, and an extra part represented extend electrodes has been added for explaination. It is

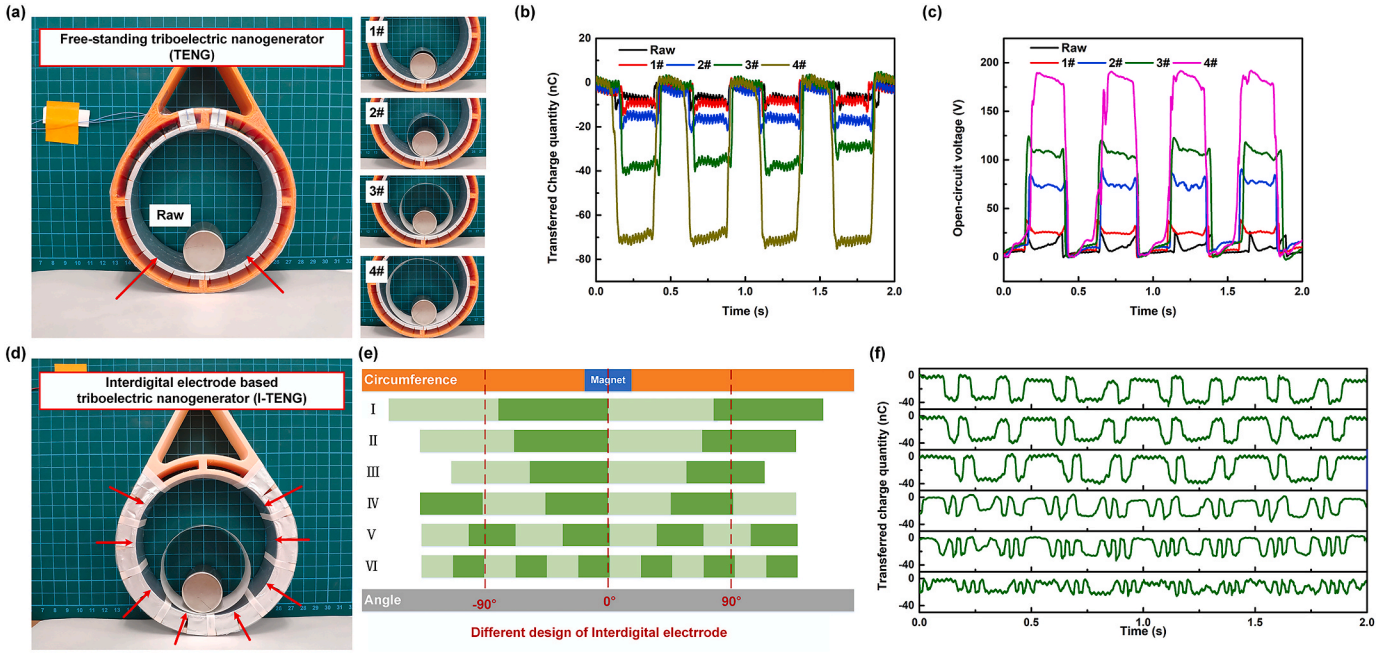

Fig. 2. (a) Photos of different sized flexible circular rings supporting a cylinder magnet, and a free-standing triboelectric nanogenerator is attached on the inner wall of the pendulum structure. (b) Transferred charge quantity with different sized rings. (c) Open circuit voltage with different sized rings. (d) Photo of the pendulum structure equipped with I-TENG and a flexible circular ring supported magnet. (e) Schematic diagram of different designs of interdigital electrodes. (f) Transferred charge quantity with different designs of interdigital electrodes.

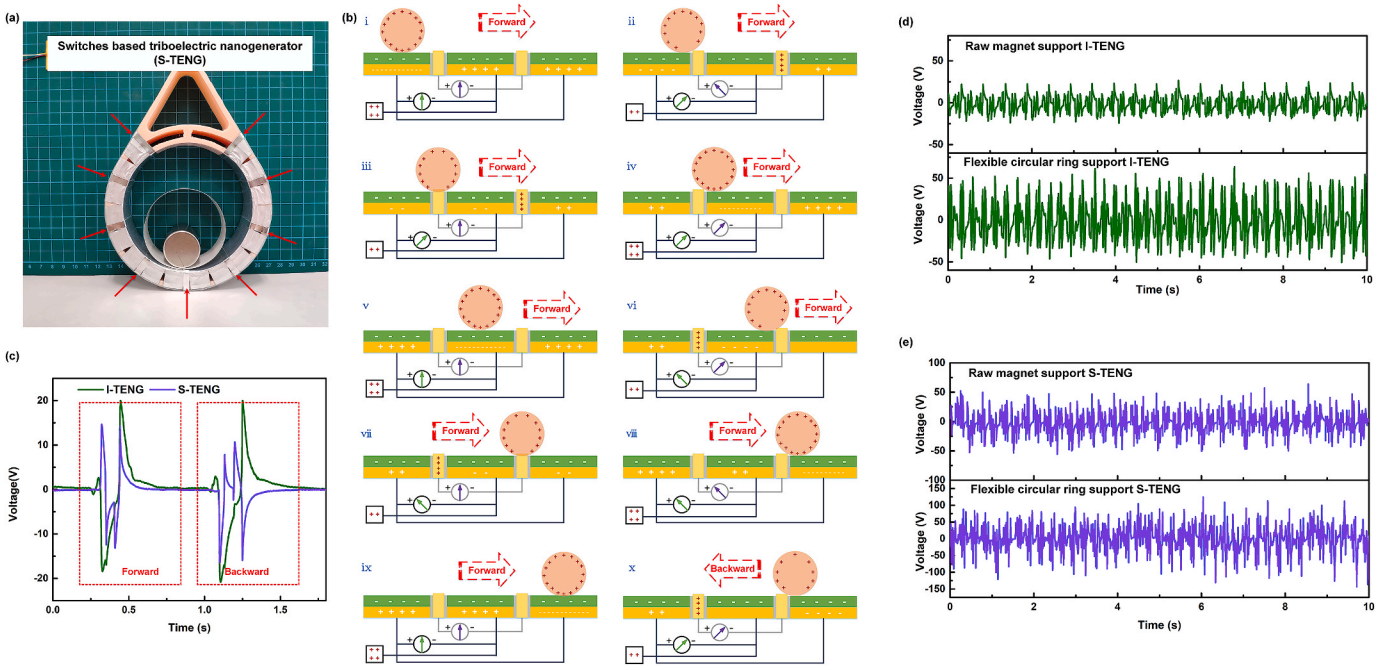

Fig. 3. (a) Photo of the pendulum structure equipped the I-TENG and the S-TENG (b) Work mechanism of the I-TENG and the S-TENG. (c) Voltage outputs when magnet rolled forward and back. (d) Outputs comparison of raw magnet based I-TENG and flexible circular ring based I-TENG. (e) Outputs comparison of raw magnet based S-TENG and flexible circular ring based S-TENG.

worth mentioning that the direction of deflection in the amperemeter is corresponding to direction of electron flow, for example that right deflection refers to electrons are flowing to right, left deflection refers to electrons are flowing to left, and none deflection refers to none electron flow. Further details can be explained with following ten steps: (1) When the magnet starts rolling forward from left, the charge balance not only exists in the system of interdigital electrodes but also the system of the magnet and switches electrodes. It can be defined as 1st electrode, 1st switch, 2nd electrode, 2nd switch and 3rd electrode from left to right. Two amperemeters are applied to detect current flow in I-TENG and S-TENG. (2) Once the magnet gradually rolls out of 1st electrode and contacts the first switch, positive charges flow from 2nd electrode to 1st electrode through the amperemeter of the I-TENG. Meanwhile, positive charges on the magnet surface flow from 1st switch to the 2nd switch through the amperemeter of the S-TENG. (3) The magnet keeps rolling and releases from 1st electrode, positive charges continue flow from 2nd electrode to 1st electrode through the amperemeter of the I-TENG. (4) When the magnet is away from 1st electrode and releasing from 1st switch, positive charges flow from 2nd switch back to the magnet's surface through the amperemeter of the S-TENG. And positive charges in 2nd electrode are keeping flowing to 1s electrode through the amperemeter of the I-TENG. (5) The charge balance is rebuilt in I-TENG's system when the magnet rolls on 2nd electrode, and positive and negative charges are redistributed to balance negative charges in dielectric film and positive charges in the magnet. (6) When the magnet continues moving forward and contacts with 2nd switch, positive charges flow from 3rd electrode to 2nd electrode through the amperemeter of the I-TENG, and flow from the magnet surface to 1st switch through the amperemeter of the S-TENG. (7) While the magnet release from 2nd electrode, positive charges continue flowing from 3rd electrodeto 2nd electrode. (8) Then the magnet continues rolling away from 2nd electrode and 2nd switch, positive charges flow from 3rd electrode to 2nd electrode through the amperemeter of the I-TENG, and flow back to the magnet's surface through the amperemeter of the S-TENG. (9) After the magnet rolls on 3rd electrode, positive and negative charges are redistributed to balance negative charges in dielectric film and positive charges in the magnet, and the charge balance is rebuilt in system. (10) Similarly, when the magnet rolls backward and contacts 2nd switch, positive charges flow from 2nd electrodes to 3rd electrode through the amperemeter of the I-TENG, and flow from the magnet surface to 1st switch through the amperemeter of the S-TENG. To sum up, the transferred charges of the I-TENG and S-TENG are benefited from the charge balance built from triboelectrification between roller and dielectric film, and charges from the roller can be utilized for energy harvesting. The voltage signals shown in Fig. 3c have proved explaination of work mechanism. Thus, the flexible circular ring discussed last parts can also applied to enhance outputs of the I-TENG and the S-TENG. Results demonstrated in Fig. 3d and e have proved effect of the flexible circular ring. Average voltages of the I-TENG and the S-TENG increase from 25 V to 52 V and increase from 45 V to 97 V respectively. Test from multiple times of rolling back and forth, the peak voltage of the I-TENG and the S-TENG can reach to 63.6 V and 124.2 V respectively. Thus, this pendulum structure can efficiently generate electricity with these designs.

Outputs of the pendulum swinging around a stationary shaft are discussed in Fig. 4 and Fig. S2. As shown in Fig. S2a, the pendulum structure containg the I-TENG, the S-TENG, the optimized flexible circular ring and the magnet is sealed with a 3D printed lid equipped with an induction coil. Then a stationary shaft is put through the pendulum and the pendulum can swing from side to side, corresponding to the photos are shown in Fig. S2b. The pendulum is operated in the air at different swing angles from equilibrium position defined in Fig. S2c and different swing frequency defined in Fig. S2d. First, results of different swing angles of 30°, 45°, 60° and 90° are demonstrated in Fig. 4a,b,c and d, and the outputs of the I-TENG, S-TENG and EMG vary in peak numbers and in peak value. The peak numbers have increased by the swing angle because that potential energy stored in the pendulum structure is improved with higher position from the equilibrium position. It can be found that there are 10 peaks from the I-TENG, 20 peaks

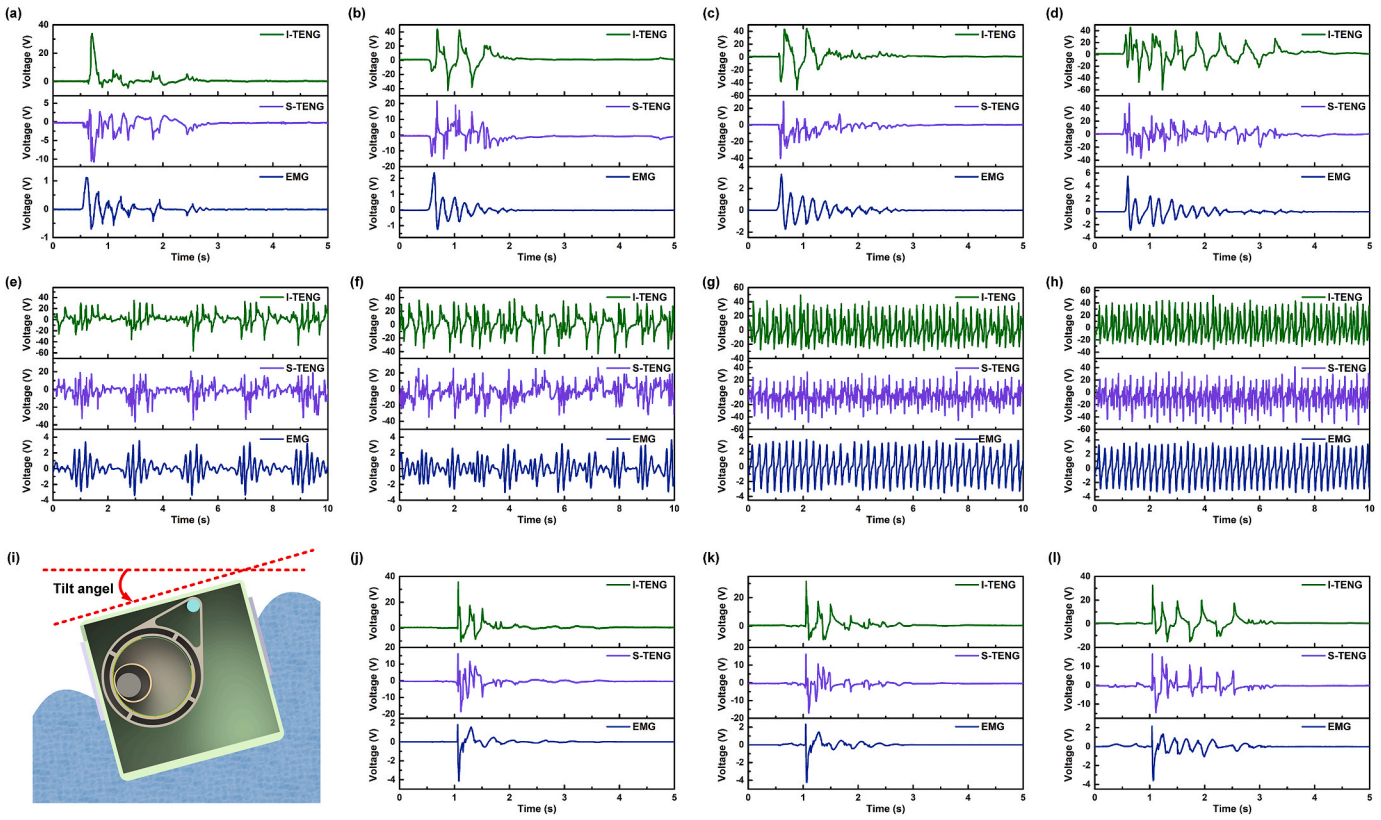

Fig. 4. (a–d) Outputs under swing angle of 30°, 45°, 60° and 90° respectively. (e–h) Outputs under swing frequency of 0.25 Hz, 0.5 Hz, 1 Hz and 2 Hz respectively. (i) Schematic diagram of operation with the hybridized blue energy harvester in the waterproof enclosed box. (j–l) Outputs of the hybridized blue energy harvester operated with swing angle of 30°, 45° and 60° respectively.

from the S-TENG and 15 peaks from the EMG during their damping process with initial angle of 90°, while only 4 peaks, 11 peaks and 7 peaks are found respectively in their damping process with initial angle of 30°. For the I-TENG, slight increments of peak value are observed when the swing angle increases due to the increment of contact between the flexible circular ring and inner surface. For the S-TENG, maximum peak value increases significantly with the swing angle because of the rapider contact with the switch electrode. Voltage outputs of the EMG are enhanced as swing angle increases, attributed to greater rolling speed of the roller. Next, swing frequency of 0.25 Hz, 0.5 Hz, 1 Hz and 2 Hz are tested to evaluate the output performance of the I-TENG, S-TENG and EMG, the results are demonstrated in Fig. 4e,f,g and h. These generators can work at both lower and higher than 1 Hz, meanwhile there is no significant decrement of outputs. Voltage outputs of the EMG shows little damping at 1 Hz and 2 Hz. Outputs at the situation of successive impacts have been illustrated in Fig. S3. There are sharp increments of voltage response to the impact have been found and damping peaks emerge when the impact is removed. Thus, this device shows the potential of harvesting wave energy featured with low frequency and successive impacts by pendulum's swing operations.

A waterproof box is applied to package the pendulum structure and a stationary shaft. As shown in Fig. 4m, this whole device can float and move with water waves due to the buoyancy foam circle attached on the box, and further tests are performed in water environment. The positions of the stationary shaft are discussed in Fig. 4i and Fig. S4, where outputs result in different responses to water waves. When the stationary shaft is placed at side position, it implies that there is more space for the pendulum's swinging. In accordance with former discussion, voltage peaks of the I-TENG, S-TENG and EMG all increase as the swing angle increases after changing the stationary shaft from middle position to side position. Another key factor of water waves' amplitude is also discussed in Fig. 4j, k and l, where whole device tilts 30°, 45° and 60° respectively. In addition, limited by box's size the pendulum's max swing angle is about 31°, so that the stored potential energy force the pendulum structure to swing back and hit the inner wall of box at situation of more than this angle. When the box waving from 45°, more voltage peaks emerge compared to the situation of 30°. When the box waves from 60°, even more voltage peaks emerge and outputs from a period of inside roller's swing have demonstrated in the outputs shown in Fig. 4l. To sum up, small wave motions lead to the swinging of the pendulum structure, strong wave motions can force the pendulum structure to hit the inner wall, resulting in higher output. Thus this packaged device has great potential to be applied as a hybridized blue energy harvester in a wide range of water wave conditions.

Energy storage circuit for the I-TENG, S-TENG and EMG is designed and discussed in Fig. 5. Corresponding tests of single-time swing and successive impacts are applied on the pendulum to value charge performance. Operations are explained in Fig. S5, where the pendulum is lift up to 90° then release for single-time swing in Fig. S5a, or the pendulum is forced to continuously swinging by successive impacts right side in Fig. S5b. First, rectifier bridges are applied to convert the AC outputs of generators into DC outputs. As shown in Fig. 5a, rectified voltages are obtained, where obvious damping is demonstrated in the voltage curves. After that, a buck circuit where the induction coil played as an inductance is applied to enhance TENGs' charging performance, as shown in Fig. 5b(i) and Fig. 5c. With the induction coil in the buck circuit, voltage of a capacitor of 1 μF can reach a higher value in single-time operation of the pendulum swinging from 90°, for all the situations

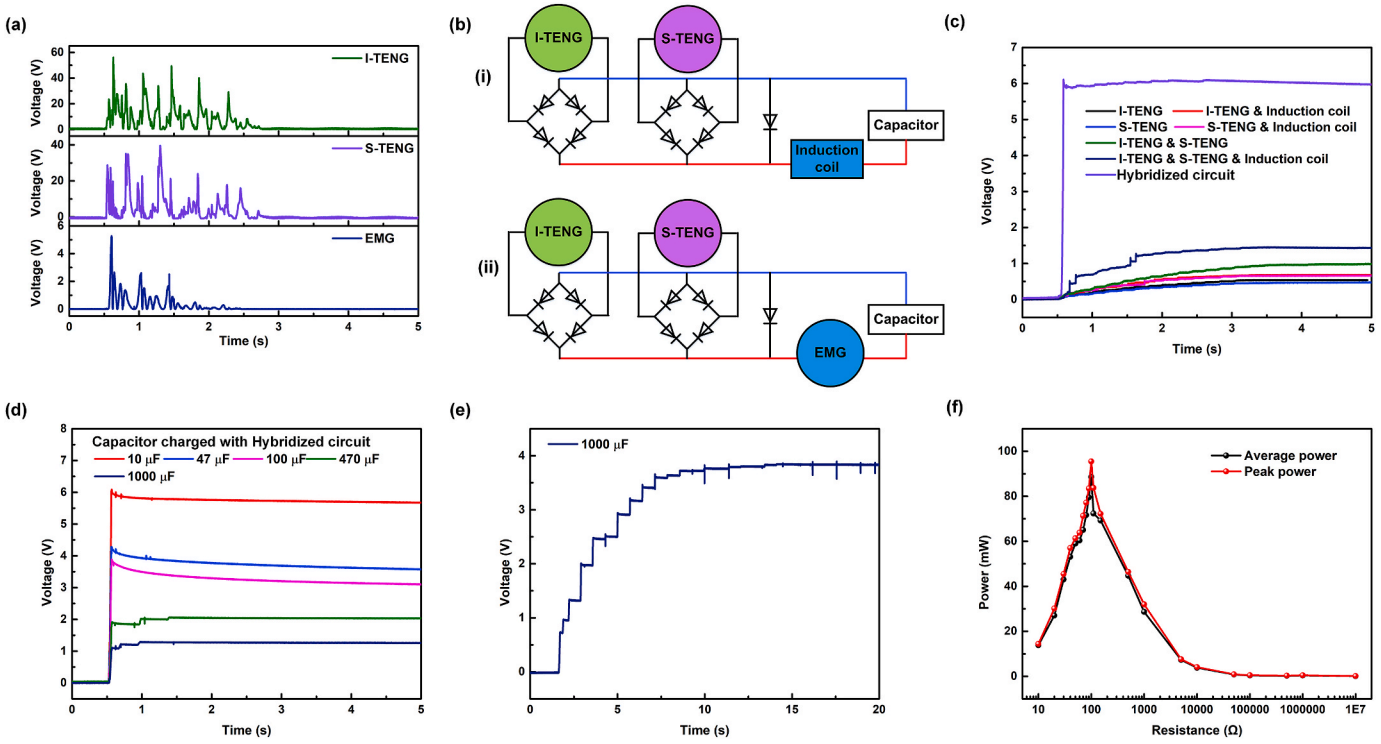

Fig. 5. (a) Outputs with rectifier bridge. (b) Design of (i) buck circuit and (ii) hybridized circuit. (c) Capacitor charging performance with and without buck circuit. (d) Capacitor charging performance with hybridized circuit. (e) A capacitor of 1000 μF was charged under successive impact of 1 Hz. (f) Output power under different load resistance.

of I-TENG, S-TENG, and I-TENG plus S-TENG. Next, a hybridized circuit shown in Fig. 5b(ii) is first introduced to support triboelectric-electromagnetic hybridized generator. A capacitor of 1 μF can reach to 6.1 V by the hybridized circuit, while it only reaches to 1.4 V by buck circuit operated with the I-TENG and the S-TENG. Moreover, different capacitors have been charged in Fig. 5d, where a capacitor of 1000 μF can be charged to 1.28 V after single-time operation of the pendulum swinging from 90°. With successive impacts of 1 Hz, a capacitor of 1000 μF can be charged to 3.7 V in 7 s by this device, and details are demonstrated in Fig. 5e. Power of this device with hybridized circuit has been calculated under different load in Fig. 5f, where peak power of this device can reach to 95.4 mW at load of 100 Ω, and relevant power density is 5.11 W/m^3. Overall, this device can extract energy with low frequency operations, and efficiently charge capacitor with hybridized circuit.

Although pendulum structure has been multiply promoted to apply

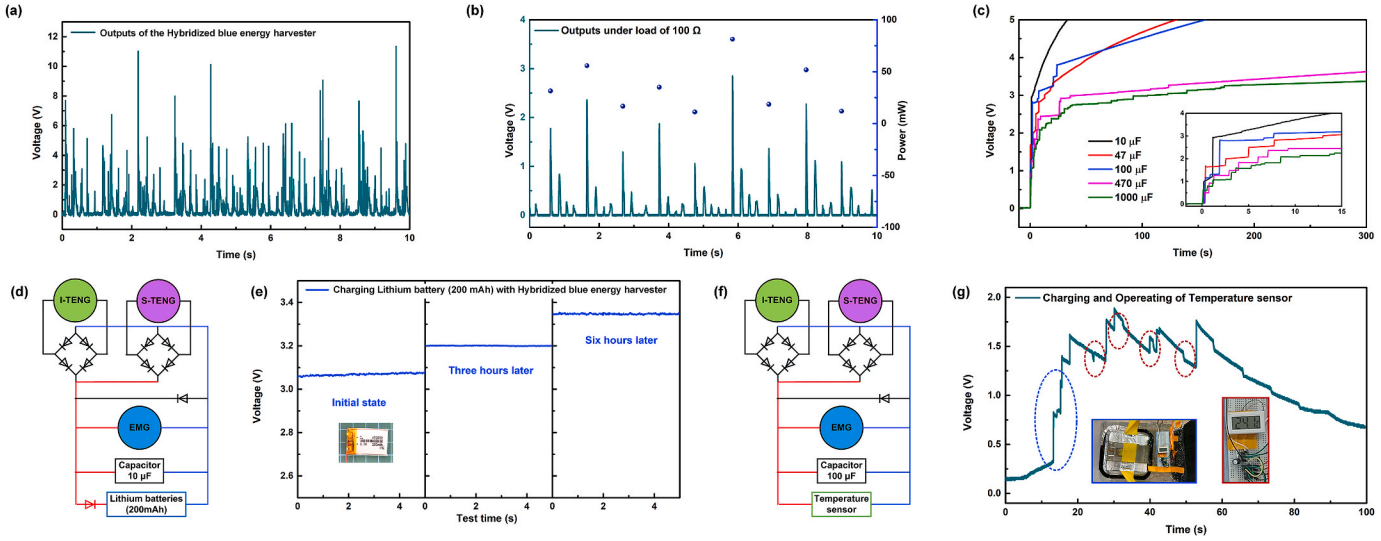

Fig. 6. (a) Outputs with hybridized circuit in waves' operation. (b) Power calculation under load of 100 Ω. (c) Capacitor charging performance with hybridized circuit in waves' operation. (d) Circuit design for lithium battery charging. (e) Circuit design for powering a temperature sensor. (f) Voltage curve as a temperature sensor was powered with the hybridized blue energy harvester and working continuously.

as energy harvester, following points can be highlighted from above discussions. Compared with latest progress reported by Yang et al. [93], the pendulum here is packaged in a waterproof box and directly operated with water waves. Moreover this prepared hybridized blue energy harvester can float with waves and extract energy from broader area. Up to similar mechanism applied with triboelectric-electromagnetic hybridized generator, the rolling magnet with a flexible circular ring help to enhance outputs, which is a newly finding and an efficient strategy about hybridized blue energy harvester. Further more, the hybridized circuit is first introduced to support hybridized blue energy harvester, and its managed power is higher than previously report of 22.5 mW.

Next, operations under 1 Hz of wave motions are applied to the hybridized blue energy harvester. As shown in Supplementary movie V1, the inside pendulum can swing with water waves. Combining the hybridized blue energy harvester with the hybridized circuit, the outputs under 1 Hz of random wave motions are further tested and illustrated in Fig. 6. As shown in Fig. 6a, multiple damping peaks appear following the impaction peak from waves, and maximum voltage reaches 11.3 V. Correspond outputs of current has been illustrated in Fig. S6, which also present multiple damping peaks. The maximum output power under load of 100 Ω can reach 81.3 mW shown in Fig. 6b, attributed to the rigid contact of the pendulum with inner wall. Then a series of capacitors is charged with the hybridized blue energy harvester in water environment, and results are demonstrated in Fig. 6c. On account of complex wave motions, capacitors can be first charged to certain voltage level rapidly attributed to the high output current from EMG, and further charged up gradually by TENGs as successive wave motions. A capacitor of 100 μF can be charged to 5 V within 160 s, and a capacitor of 1000 μF can be charged to 3.26 V within 180 s. Along with successive waves, that capacitor of 1000 μF can be further charged to 3.4 V within 300 s.

Supplementary video related to this article can be found at https://doi.org/10.1016/j.nanoen.2020.105052.

Further applications of charging lithium battery and powering temperature sensor are also investigated to demonstrate the charging capability of this hybridized blue energy harvester. As shown in Fig. 6d and e, corresponding battery charging circuit is introduced with a diode to prevent reverse current from the lithium battery to the capacitor. With a wave pump at pool's bottom, a lithium battery of 200 mAh can be charged from 3.07 V to 3.35 V within six hours. To clarify, although the lithium battery is widespread used and closer to practical applications than capacitors, few reported blue energy harvesters are applied to charge it. Compared with latest progress from Gao et. Al., [92], here a lithium battery with larger capacity is charged under water waves instead of mechanical motor. Moreover, a digital temperature sensor with a temperature detector immersed in the water can be continuously powered in Fig. 6f and g. Attributed to efficient outputs of this hybridized energy harvester, the sensor is waked up by waves and can work continuously, which is also shown in Supplementary movie V2. This temperature sensor equipped with a display screen can directly transfer message to observer, and a temperature probe with long wire can detect remote temperature signals.

Supplementary video related to this article can be found at https://doi.org/10.1016/j.nanoen.2020.105052.

To cope with capricious climate around ocean area, ability of working in all-weather situations shows importance to the blue energy harvester. Compared reported all-weather device from Liu et al. [56], a more representative all-weather IoT platform is promoted with a Bluetooth sensor module. This Bluetooth sensor module shown in Fig. 7 can monitor the ambient temperature and humidity, and then transmit these sensory signals to the user-end of a mobile phone. Original operation with solar cell is shown in Fig. S7, where that Bluetooth sensor module can not work under darkness condition. With the integration of the hybridized blue energy harvester with the amorphous silicon solar cell panel (15 mm*15 mm), an all-weather self-powered IoT node is introduced and shown in Fig. 7a and b. In the situation of daylight without waves, the Bluetooth sensor module is powered by the solar cell individually. With the regular operation voltage of 3.3 V and relatively long charging period of solar cell, sensing signals can only be transmitted four times within 200 s, with a average operation time of 45 s for signal-time transmission. Details are shown in Fig. 7c, once the voltage reaches 3.3 V the Bluetooth sensor module will start to work, and the voltage drops down to 1.8 V. In the situation of darkness with waves displayed in Fig. S8, the solar cell panel is coved with a sheet of black tape. The Bluetooth sensor module is powered with the hybridized blue energy harvester shown in Fig. 7d, where the signals can be transmitted eight times within 200 s due to efficient conversion of water wave energy with a average operation time of 23 s for signal-time transmission, which is twice the transmission rate with only solar cell. In the situation of daylight with waves shown in Fig. 7e, signals have been transmitted nine

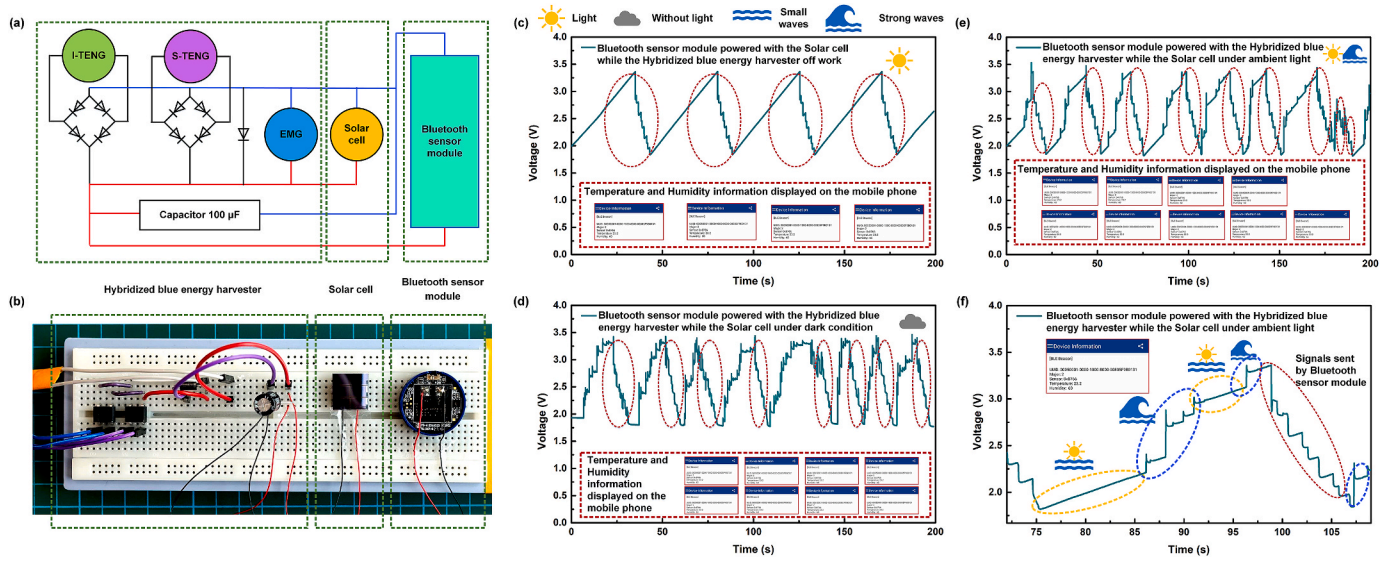

Fig. 7. (a) Circuit design of an all-weather IoT application. (b) Photo of circuit contains a solar cell panel and a Bluetooth sensor module. (c) Voltage curve as the Bluetooth sensor module powered with the solar cell. (d) Voltage curve as the Bluetooth sensor module powered with the hybridized blue energy harvester. (e) Voltage curve as the Bluetooth sensor module powered with the hybridized blue energy harvester and the solar cell. (f) Details about one-time wireless signals transmission.

times within 200 s, with a average operation time of 22 s for signal-time transmission. All above mentioned signals displayed on the mobile phone are enlarged and shown in Fig. S9. A typical process has been selected from Fig. 7e to explain working mechanism, and it is demonstrated in Fig. 7f. The voltage is gradually increased with solar cell under daylight and tiny small wave, but abruptly increased with the hybridized blue energy harvester under daylight and strong waves. These three situations have also been demonstrated in Supplementary movie V3-5, showing that the all-weather IoT application can be achieved.

Supplementary video related to this article can be found at https://doi.org/10.1016/j.nanoen.2020.105052.

3. Conclusion

In summary, a hybridized blue energy harvester has been designed and fabricated based on the integration of triboelectric nanogenerators and electromagnetic generator. Wherein a pendulum structure, containing the interdigital electrodes-TENG, the switches-TENG and the EMG, is packaged in a waterproof enclosed box. The outputs of TENGs are enhanced by an optimized flexible circular ring supporting a rolling magnet. In the wave test, a capacitor of 1000 μF is charged to 3.26 V within 180 s with wave motions, and a lithium battery (200 mAh) have been charged from 3.07 V to 3.35 V with six hours of water wave impaction. Besides of directly and continuously power a digital temperature sensor with the hybridized blue energy harvester, an all-weather IoT platform is also established with the blue energy harvester, a solar cell panel and a Bluetooth low energy sensor. The ambient information of humidity and temperature can be detected and sent to user-end by the Bluetooth sensor module under various conditions with or without daylight and water waves. Moreover, the signals also can be sent and received eight times in 200 s under the situation of darkness benefit by the blue energy harvester operated in water waves, where the transmission rate is double of that only with solar cell operation. Thus, this hybridized blue energy harvester can effectively extract water wave energy and demonstrates promising potentials in battery-free IoT applications in ocean area.

4. Experimental section

4.1. Fabrication of the Triboelectric–Electromagnetic hybridized generator

Firstly, the rigid structures including pendulum structure and lid parts are prepared by the 3D printer (ANYCUBIC 4Max Pro) with polylactic acid (PLA). Note that the pendulum structure has a radial dimension of 35 mm and a wall thickness of 3 mm, and the lid parts' thickness is 5 mm with a circular hole of 2 mm depth. After moderate sanding and refinishing, the pendulum structure inner side is attached VHB super strong double-sided tape (3 M) of 35 mm width. And the lid parts is covered plastic film to reduce drag of the rolling magnet. Secondly, A sheet of FEP (50 μm thickness, 10 cm width, DUPONT) attached with Aluminum tape are cut into different sizes (7*10 cm, 6*10 cm,5*10 cm,4*10 cm,3*10 cm, 2*10 cm). Thirdly, these pieces are pasted in turns at intervals of 1 mm from the middle-bottom line of the pendulum structure. Extra parts of these pieces are fixed to the rigid margin and corresponding interdigital electrodes are linked with wires outside of the pendulum structure. Fourthly, strips of Aluminum tape with release paper (2 mm*10 cm) are stuck to cover the intervals between interdigital electrodes, and extra parts are also fixed to the rigid margin and corresponding electrodes are linked with wires outside of the pendulum structure. Fifthly, a sheet of Aluminum tape with released paper (3 cm width) are cut into different sizes (10 cm*3 cm, 15 cm*3 cm, 20 cm*3 cm, 25 cm*3 cm), then ends of these pieces are connected and turned into circular rings with different sizes. Finally, the cylindrical magnet (3 cm of diameter, 3 cm of length) with a flexible circular ring is encapsulated in the pendulum structure with lids, and an induction coil (46 mm of diameter, 10 mm of inner diameter, 51.5 mH) is fixed in the circular hole of the lid. Then the whole device is reinforced with rubber rings and adhesive tapes, and whole size of X*Y*Z direction is 12.6 cm*17.5 cm *4.6 cm.

4.2. Fabrication of the hybridized blue energy harvester

A waterproof box (CRYSTALPAK wafer shipping box) is chosen to hold the Triboelectric–Electromagnetic Hybridized Generator. The specific operation is as follows, firstly a stainless-steel rod (20 mm length, 6 mm diameter) played as the stationary shaft through the pendulum structure of the triboelectric–electromagnetic hybridized generator, then fastened in the upper part of the box. Note that a sticky tape help limit the triboelectric–electromagnetic hybridized generator in the middle area while the generator still can rotation around the rod. After sealing this box, a round of EVA float foam (11 cm width, 2.5 cm thickness) is fixed at upper part of the box to guarantee the box not inversion in varying waves environment. Note that a stretch band (0.25 mm thickness) is used to keep the hybridized blue energy harvester off floating away while waving testing. The testing pool (52 cm length, 70 cm width, 43 cm height) contains 45 L of water, and a pump wave pump (Laoyujiang) is equipped on bottom of box.

4.3. Characterization and electrical measurement

The open-circuit voltage, charge quantity and capacitor's voltage are measured by Electrometer (Keithley Model 6514), and experiments' data is acquired and saved by Model DSOX3034T Oscilloscope (Keysight). The outputs of voltage are tested and acquired by 1X probe (GTL-101) and 1000X probe (TT-HVP-15HF).

Declaration of competing interest

The authors declare that they have no known competing financial interests or personal relationships that could have appeared to influence the work reported in this paper.

CRediT authorship contribution statement

Long Liu: Conceptualization, Data curation, Formal analysis, Investigation, Methodology, Resources, Software, Validation, Visualization, Writing - original draft, Writing - review & editing. **Qiongfeng Shi:** Investigation, Validation, Formal analysis, Visualization, Writing - review & editing. **Chengkuo Lee:** Conceptualization, Methodology, Supervision, Project administration, Funding acquisition, Writing - review & editing.

Acknowledgements

This work was supported by: HIFES Seed Funding-2017-01 grant (R263-501-012-133) "Hybrid Integration of Flexible Power Source and Pressure Sensors" at the National University of Singapore. NRF-ISF Seed Funding (R-263-000-C64-281) "Reconfigurable data center optical interconnects using fast nanophotonic MEMS waveguide switches". Singapore-Poland Joint Grant (R-263-000-C91-305) "Chip-Scale MEMS MicroSpectrometer for Monitoring Harsh Industrial Gases" by Agency for Science, Technology and Research (A*STAR), Singapore and NAWA"Academic International Partnerships of Wroclaw University of Science and technology" programme by Polish National Agency for Academic Exchange Programme.

Appendix A. Supplementary data

Supplementary data to this article can be found online at https://doi.org/10.1016/j.nanoen.2020.105052.

References

[1] Q. Schiermeier, J. Tollefson, T. Scully, A. Witze, O. Morton, Energy alternatives: electricity without carbon, Nature 454 (2008) 816–823.
[2] D. Gielen, F. Boshell, D. Saygin, Climate and energy challenges for materials science, Nat. Mater. 15 (2016) 117–120.
[3] J.A. Turner, A realizable renewable energy future, Science 285 (1999) 687–689.
[4] J. Tollefson, Power from the oceans: blue energy, Nature 508 (2014) 302–304.
[5] J. Scruggs, P. Jacob, Harvesting ocean wave energy, Science 323 (2009) 1176–1178.
[6] M.A. Mustapa, O.B. Yaakob, Y.M. Ahmed, C.-K. Rheem, K.K. Koh, F.A. Adnan, Wave energy device and breakwater integration: a review, Renew. Sustain. Energy Rev. 77 (2017) 43–58.
[7] AFdO. Falcão, Wave energy utilization: a review of the technologies, Renew. Sustain. Energy Rev. 14 (2010) 899–918.
[8] Z.L. Wang, Catch wave power in floating nets, Nature 542 (2017) 159–160.
[9] Z.L. Wang, T. Jiang, L. Xu, Toward the blue energy dream by triboelectric nanogenerator networks, Nano Energy 39 (2017) 9–23.
[10] C. Wu, A.C. Wang, W. Ding, H. Guo, Z.L. Wang, Triboelectric nanogenerator: a foundation of the energy for the new era, Adv. Energy Mater. 9 (2019) 1802906.
[11] T. Jingwen, C. Xiangyu, W. Zhong Lin, Environmental energy harvesting based on triboelectric nanogenerator, Nanotechnology 31 (24) (2020) 242001.
[12] H. Chen, C. Xing, Y. Li, J. Wang, Y. Xu, Triboelectric nanogenerators for a macro-scale blue energy harvesting and self-powered marine environmental monitoring system, Sustain. Energy Fuels 4 (2020) 1063–1077.
[13] Y. Zi, Z.L. Wang, Nanogenerators: an emerging technology towards nanoenergy, Apl. Mater. 5 (2017), 074103.
[14] L. Liu, Q. Shi, J.S. Ho, C. Lee, Study of thin film blue energy harvester based on triboelectric nanogenerator and seashore IoT applications, Nano Energy 66 (2019) 104167.
[15] Z.L. Wang, On Maxwell's displacement current for energy and sensors: the origin of nanogenerators, Mater. Today 20 (2017) 74–82.
[16] C. Xu, B. Zhang, A.C. Wang, H. Zou, G. Liu, W. Ding, C. Wu, M. Ma, P. Feng, Z. Lin, Z.L. Wang, Contact-Electrification between two identical materials: curvature effect, ACS Nano 13 (2019) 2034–2041.
[17] Z.L. Wang, Triboelectric nanogenerators as new energy technology and self-powered sensors – principles, problems and perspectives, Faraday Discuss 176 (2014) 447–458.
[18] Y. Zi, S. Niu, J. Wang, Z. Wen, W. Tang, Z.L. Wang, Standards and figure-of-merits for quantifying the performance of triboelectric nanogenerators, Nat. Commun. 6 (2015) 8376.
[19] Y. Zi, J. Wang, S. Wang, S. Li, Z. Wen, H. Guo, Z.L. Wang, Effective energy storage from a triboelectric nanogenerator, Nat. Commun. 7 (2016) 10987.
[20] Z.L. Wang, Triboelectric nanogenerator (TENG)—sparking an energy and sensor revolution, Adv. Energy Mater. n/a (2020), 2000137.
[21] L.F. Chen, Q.F. Shi, Y.J. Sun, T. Nguyen, C. Lee, S. Soh, Controlling surface charge generated by contact electrification: strategies and applications, Adv. Mater. 30 (2018).
[22] L. Dhakar, F.E.H. Tay, C. Lee, Investigation of contact electrification based broadband energy harvesting mechanism using elastic PDMS microstructures, J. Micromech. Microeng. 24 (2014) 104002.
[23] Y. Zi, H. Guo, Z. Wen, M.-H. Yeh, C. Hu, Z.L. Wang, Harvesting low-frequency (<5 Hz) irregular mechanical energy: a possible killer application of triboelectric nanogenerator, ACS Nano 10 (2016) 4797–4805.
[24] C. Zhang, W. Tang, C. Han, F. Fan, Z.L. Wang, Theoretical comparison, equivalent transformation, and conjunction operations of electromagnetic induction generator and triboelectric nanogenerator for harvesting mechanical energy, Adv. Mater. 26 (2014) 3580–3591.
[25] F.-R. Fan, W. Tang, Y. Yao, J. Luo, C. Zhang, Z.L. Wang, Complementary power output characteristics of electromagnetic generators and triboelectric generators, Nanotechnology 25 (2014) 135402 (Eye motion triggered self-powered mechnosensational communication system using triboelectric nanogenerator).
[26] Yang J, Yang S, Guo R, Li Y, Sang S, Zhang H. 1D triboelectric nanogenerator operating by repeatedly stretching and as a self-powered electronic fence and geological monitor. Adv. Mater. Technol. 2020; 5: 1901005.
[27] T. Zhao, S. Cao, S. Yang, R. Guo, S. Sang, H. Zhang, A self-powered counter/timer based on a clock pointer-like frequency-tunable triboelectric nanogenerator for wind speed detecting, Nano Energy 65 (2019) 104025.
[28] J. Chen, Z.L. Wang, Reviving vibration energy harvesting and self-powered sensing by a triboelectric nanogenerator, Joule 1 (2017) 480–521.
[29] Q. He, Y. Wu, Z. Feng, W. Fan, Z. Lin, C. Sun, Z. Zhou, K. Meng, W. Wu, J. Yang, An all-textile triboelectric sensor for wearable teleoperated human–machine interaction, J. Mater. Chem. 7 (2019) 26804–26811.
[30] P. Bai, G. Zhu, Z.-H. Lin, Q. Jing, J. Chen, G. Zhang, J. Ma, Z.L. Wang, Integrated multilayered triboelectric nanogenerator for harvesting biomechanical energy from human motions, ACS Nano 7 (2013) 3713–3719.
[31] S. Wang, Y. Xie, S. Niu, L. Lin, Z.L. Wang, Freestanding triboelectric-layer-based nanogenerators for harvesting energy from a moving object or human motion in contact and non-contact modes, Adv. Mater. 26 (2014) 2818–2824.
[32] Z. Lin, Y. Wu, Q. He, C. Sun, E. Fan, Z. Zhou, M. Liu, W. Wei, J. Yang, An airtight-cavity-structural triboelectric nanogenerator-based insole for high performance biomechanical energy harvesting, Nanoscale 11 (2019) 6802–6809.
[33] B. Shi, Z. Li, Y. Fan, Implantable energy-harvesting devices, Adv. Mater. 30 (2018) 1801511.
[34] C. Deng, W. Tang, L. Liu, B. Chen, M. Li, Z.L. Wang, Self -powered insole plantar pressure mapping system, Adv. Funct. Mater. 28 (2018) 1801606.
[35] Q. Tang, M.-H. Yeh, G. Liu, S. Li, J. Chen, Y. Bai, L. Feng, M. Lai, K.-C. Ho, H. Guo, C. Hu, Whirligig-inspired triboelectric nanogenerator with ultrahigh specific output as reliable portable instant power supply for personal health monitoring devices, Nano Energy 47 (2018) 74–80.
[36] X. Pu, H. Guo, J. Chen, X. Wang, Y. Xi, C. Hu, Z.L. Wang, Eye motion triggered self-powered mechnosensational communication system using triboelectric nanogenerator, Sci. Adv. 3 (2017), e1700694.
[37] Y. Yang, H. Zhang, R. Liu, X. Wen, T.-C. Hou, Z.L. Wang, Fully enclosed triboelectric nanogenerators for applications in water and harsh environments, Adv. Energy Mater. 3 (2013) 1563–1568.
[38] L. Xu, T. Jiang, P. Lin, J.J. Shao, C. He, W. Zhong, X.Y. Chen, Z.L. Wang, Coupled triboelectric nanogenerator networks for efficient water wave energy harvesting, ACS Nano 12 (2018) 1849–1858.
[39] T.X. Xiao, X. Liang, T. Jiang, L. Xu, J.J. Shao, J.H. Nie, Y. Bai, W. Zhong, Z. L. Wang, Spherical triboelectric nanogenerators based on spring-assisted multilayered structure for efficient water wave energy harvesting, Adv. Funct. Mater. 28 (2018) 1802634.
[40] G. Zhu, Y. Su, P. Bai, J. Chen, Q. Jing, W. Yang, Z.L. Wang, Harvesting water wave energy by asymmetric screening of electrostatic charges on a nanostructured hydrophobic thin-film surface, ACS Nano 8 (2014) 6031–6037.
[41] M. Xu, S. Wang, S.L. Zhang, W. Ding, P.T. Kien, C. Wang, Z. Li, X. Pan, Z.L. Wang, A highly-sensitive wave sensor based on liquid-solid interfacing triboelectric nanogenerator for smart marine equipment, Nano Energy 57 (2019) 574–580.
[42] X. Yang, L. Xu, P. Lin, W. Zhong, Y. Bai, J. Luo, J. Chen, Z.L. Wang, Macroscopic self-assembly network of encapsulated high-performance triboelectric nanogenerators for water wave energy harvesting, Nano Energy 60 (2019) 404–412.
[43] T. Jiang, Y. Yao, L. Xu, L. Zhang, T. Xiao, Z.L. Wang, Spring-assisted triboelectric nanogenerator for efficiently harvesting water wave energy, Nano Energy 31 (2017) 560–567.
[44] S.L. Zhang, M. Xu, C. Zhang, Y.-C. Wang, H. Zou, X. He, Z. Wang, Z.L. Wang, Rationally designed sea snake structure based triboelectric nanogenerators for effectively and efficiently harvesting ocean wave energy with minimized water screening effect, Nano Energy 48 (2018) 421–429.
[45] J. Tan, J. Duan, Y. Zhao, B. He, Q. Tang, Generators to harvest ocean wave energy through electrokinetic principle, Nano Energy 48 (2018) 128–133.
[46] Z.-H. Lin, G. Cheng, S. Lee, K.C. Pradel, Z.L. Wang, Harvesting water drop energy by a sequential contact-electrification and electrostatic-induction process, Adv. Mater. 26 (2014) 4690–4696.
[47] Z.-H. Lin, G. Cheng, L. Lin, S. Lee, Z.L. Wang, Water–Solid surface contact electrification and its use for harvesting liquid-wave energy, Angew. Chem. Int. Ed. 52 (2013) 12545–12549.
[48] Z.-H. Lin, G. Cheng, W. Wu, K.C. Pradel, Z.L. Wang, Dual-mode triboelectric nanogenerator for harvesting water energy and as a self-powered ethanol nanosensor, ACS Nano 8 (2014) 6440–6448.
[49] A. Ahmed, Z. Saadatnia, I. Hassan, Y. Zi, Y. Xi, X. He, J. Zu, Z.L. Wang, Self-powered wireless sensor node enabled by a duck-shaped triboelectric nanogenerator for harvesting water wave energy, Adv. Energy Mater. 7 (2017) 1601705.
[50] T. Jiang, L.M. Zhang, X. Chen, C.B. Han, W. Tang, C. Zhang, L. Xu, Z.L. Wang, Structural optimization of triboelectric nanogenerator for harvesting water wave energy, ACS Nano 9 (2015) 12562–12572.
[51] W. Liu, L. Xu, T. Bu, H. Yang, G. Liu, W. Li, Y. Pang, C. Hu, C. Zhang, T. Cheng, Torus structured triboelectric nanogenerator array for water wave energy harvesting, Nano Energy 58 (2019) 499–507.
[52] Z. Lin, B. Zhang, H. Guo, Z. Wu, H. Zou, J. Yang, Z.L. Wang, Super-robust and frequency-multiplied triboelectric nanogenerator for efficient harvesting water and wind energy, Nano Energy 64 (2019) 103908.
[53] Z. Lin, B. Zhang, H. Zou, Z. Wu, H. Guo, Y. Zhang, J. Yang, Z.L. Wang, Rationally designed rotation triboelectric nanogenerators with much extended lifetime and durability, Nano Energy 68 (2020) 104378.
[54] L. Pan, J. Wang, P. Wang, R. Gao, Y.-C. Wang, X. Zhang, J.-J. Zou, Z.L. Wang, Liquid-FEP-based U-tube triboelectric nanogenerator for harvesting water-wave energy, Nano Res. 11 (2018) 4062–4073.
[55] P. Cheng, H. Guo, Z. Wen, C. Zhang, X. Yin, X. Li, D. Liu, W. Song, X. Sun, J. Wang, Z.L. Wang, Largely enhanced triboelectric nanogenerator for efficient harvesting of water wave energy by soft contacted structure, Nano Energy 57 (2019) 432–439.
[56] G. Liu, H. Guo, S. Xu, C. Hu, Z.L. Wang, Oblate spheroidal triboelectric nanogenerator for all-weather blue energy harvesting, Adv. Energy Mater. 9 (2019) 1900801.
[57] P. Cheng, Y. Liu, Z. Wen, H. Shao, A. Wei, X. Xie, C. Chen, Y. Yang, M. Peng, Q. Zhuo, X. Sun, Atmospheric pressure difference driven triboelectric nanogenerator for efficiently harvesting ocean wave energy, Nano Energy 54 (2018) 156–162.
[58] Q. Tang, X. Pu, Q. Zeng, H. Yang, J. Li, Y. Wu, H. Guo, Z. Huang, C. Hu, A strategy to promote efficiency and durability for sliding energy harvesting by designing alternating magnetic stripe arrays in triboelectric nanogenerator, Nano Energy 66 (2019) 104087.
[59] X. Li, J. Tao, X. Wang, J. Zhu, C. Pan, Z.L. Wang, Networks of high performance triboelectric nanogenerators based on liquid–solid interface contact electrification for harvesting low-frequency blue energy, Adv. Energy Mater. 8 (2018) 1800705.
[60] W. Tang, B.D. Chen, Z.L. Wang, Recent progress in power generation from water/liquid droplet interaction with solid surfaces, Adv. Funct. Mater. 29 (2019) 1901069.

[61] H. Zou, Y. Zhang, L. Guo, P. Wang, X. He, G. Dai, H. Zheng, C. Chen, A.C. Wang, C. Xu, Z.L. Wang, Quantifying the triboelectric series, Nat. Commun. 10 (2019) 1427.
[62] L. Liu, W. Tang, Z.L. Wang, Inductively-coupled-plasma-induced electret enhancement for triboelectric nanogenerators, Nanotechnology 28 (2016), 035405.
[63] L. Dhakar, F.E.H. Tay, C. Lee, Development of a broadband triboelectric energy harvester with SU-8 micropillars, J. Microelectromech. Syst. 24 (2015) 91–99.
[64] L. Dhakar, S. Gudla, X. Shan, Z. Wang, F.E.H. Tay, C.-H. Heng, C. Lee, Large scale triboelectric nanogenerator and self-powered pressure sensor array using low cost roll-to-roll UV embossing, Sci. Rep. 6 (2016) 22253.
[65] K. Xia, Z. Zhu, H. Zhang, C. Du, R. Wang, Z. Xu, High output compound triboelectric nanogenerator based on paper for self-powered height sensing system, IEEE Trans. Nanotechnol. 17 (2018) 1217–1223.
[66] F. Xi, Y. Pang, W. Li, T. Jiang, L. Zhang, T. Guo, G. Liu, C. Zhang, Z.L. Wang, Universal power management strategy for triboelectric nanogenerator, Nano Energy 37 (2017) 168–176.
[67] X. Liang, T. Jiang, G. Liu, T. Xiao, L. Xu, W. Li, F. Xi, C. Zhang, Z.L. Wang, Triboelectric nanogenerator networks integrated with power management module for water wave energy harvesting, Adv. Funct. Mater. 29 (2019) 1807241.
[68] Y. Yao, T. Jiang, L. Zhang, X. Chen, Z. Gao, Z.L. Wang, Charging system optimization of triboelectric nanogenerator for water wave energy harvesting and storage, ACS Appl. Mater. Interfaces 8 (2016) 21398–21406.
[69] X. Liang, T. Jiang, G. Liu, Y. Feng, C. Zhang, Z.L. Wang, Spherical triboelectric nanogenerator integrated with power management module for harvesting multidirectional water wave energy, Energy Environ. Sci. 13 (2020) 277–285.
[70] H.C. Liu, J.W. Zhong, C. Lee, S.W. Lee, L.W. Lin, A comprehensive review on piezoelectric energy harvesting technology: materials, mechanisms, and applications, Appl. Phys. Rev. 5 (2018).
[71] H. Liu, K. How Koh, C. Lee, Ultra-wide frequency broadening mechanism for micro-scale electromagnetic energy harvester, Appl. Phys. Lett. 104 (2014), 053901.
[72] H. Liu, C. Quan, C.J. Tay, T. Kobayashi, C. Lee, A MEMS-based piezoelectric cantilever patterned with PZT thin film array for harvesting energy from low frequency vibrations, Phys. Procedia 19 (2011) 129–133.
[73] R.K. Gupta, Q. Shi, L. Dhakar, T. Wang, C.H. Heng, C. Lee, Broadband energy harvester using non-linear polymer spring and electromagnetic/triboelectric hybrid mechanism, Sci. Rep. 7 (2017) 41396.
[74] K. Zhang, Y. Wang, Y. Yang, Structure design and performance of hybridized nanogenerators, Adv. Funct. Mater. 29 (2019) 1806435.
[75] K. Song, R. Zhao, Z.L. Wang, Y. Yang, Conjuncted pyro-piezoelectric effect for self-powered simultaneous temperature and pressure sensing, Adv. Mater. 31 (2019) 1902831.
[76] Y. Wu, X. Wang, Y. Yang, Z.L. Wang, Hybrid energy cell for harvesting mechanical energy from one motion using two approaches, Nano Energy 11 (2015) 162–170.
[77] T. Quan, X. Wang, Z.L. Wang, Y. Yang, Hybridized electromagnetic–triboelectric nanogenerator for a self-powered electronic watch, ACS Nano 9 (2015) 12301–12310.
[78] X. Zhong, Y. Yang, X. Wang, Z.L. Wang, Rotating-disk-based hybridized electromagnetic-triboelectric nanogenerator for scavenging biomechanical energy as a mobile power source, Nano Energy 13 (2015) 771–780.
[79] X. Wang, Y. Yang, Effective energy storage from a hybridized electromagnetic-triboelectric nanogenerator, Nano Energy 32 (2017) 36–41.
[80] T. Quan, Y. Yang, Fully enclosed hybrid electromagnetic–triboelectric nanogenerator to scavenge vibrational energy, Nano Res. 9 (2016) 2226–2233.
[81] C. Yan, Y. Gao, S. Zhao, S. Zhang, Y. Zhou, W. Deng, Z. Li, G. Jiang, L. Jin, G. Tian, T. Yang, X. Chu, D. Xiong, Z. Wang, Y. Li, W. Yang, J. Chen, A linear-to-rotary hybrid nanogenerator for high-performance wearable biomechanical energy harvesting, Nano Energy 67 (2020) 104235.
[82] M.T. Rahman, S.M.S. Rana, M. Salauddin, P. Maharjan, T. Bhatta, J.Y. Park, Biomechanical energy-driven hybridized generator as a universal portable power source for smart/wearable electronics, Adv. Energy Mater. n/a (2020) 1903663.
[83] L. Liu, W. Tang, B. Chen, C. Deng, W. Zhong, X. Cao, Z.L. Wang, A self-powered portable power bank based on a hybridized nanogenerator, Adv. Mater. Technol. 3 (2018) 1700209.
[84] L. Liu, W. Tang, C. Deng, B. Chen, K. Han, W. Zhong, Z.L. Wang, Self-powered versatile shoes based on hybrid nanogenerators, Nano Res. 11 (2018) 3972–3978.
[85] P. Tan, Q. Zheng, Y. Zou, B. Shi, D. Jiang, X. Qu, H. Ouyang, C. Zhao, Y. Cao, Y. Fan, Z.L. Wang, Z. Li, A battery-like self-charge universal module for motional energy harvest, Adv. Energy Mater. 9 (2019) 1901875.
[86] J. He, X. Fan, J. Mu, C. Wang, J. Qian, X. Li, X. Hou, W. Geng, X. Wang, X. Chou, 3D full-space triboelectric-electromagnetic hybrid nanogenerator for high-efficient mechanical energy harvesting in vibration system, Energy 194 (2020) 116871.
[87] H. Lee, R. Sriramdas, P. Kumar, M. Sanghadasa, M.G. Kang, S. Priya, Maximizing power generation from ambient stray magnetic fields around smart infrastructures enabling self-powered wireless devices, Energy Environ. Sci. (2020), https://doi.org/10.1039/C9EE03902C.
[88] B. Chen, Y. Yang, Z.L. Wang, Scavenging wind energy by triboelectric nanogenerators, Adv. Energy Mater. 8 (2018) 1702649.
[89] P. Wang, L. Pan, J. Wang, M. Xu, G. Dai, H. Zou, K. Dong, Z.L. Wang, An ultra-low-friction triboelectric–electromagnetic hybrid nanogenerator for rotation energy harvesting and self-powered wind speed sensor, ACS Nano 12 (2018) 9433–9440.
[90] X. Fan, J. He, J. Mu, J. Qian, N. Zhang, C. Yang, X. Hou, W. Geng, X. Wang, X. Chou, Triboelectric-electromagnetic hybrid nanogenerator driven by wind for self-powered wireless transmission in Internet of Things and self-powered wind speed sensor, Nano Energy 68 (2020) 104319.
[91] X. Li, X. Yin, Z. Zhao, L. Zhou, D. Liu, C. Zhang, C. Zhang, W. Zhang, S. Li, J. Wang, Z.L. Wang, Long-Lifetime triboelectric nanogenerator operated in conjunction modes and low crest factor, Adv. Energy Mater. 10 (2020) 1903024.
[92] L. Gao, S. Lu, W. Xie, X. Chen, L. Wu, T. Wang, A. Wang, C. Yue, D. Tong, W. Lei, H. Yu, X. He, X. Mu, Z.L. Wang, Y. Yang, A self-powered and self-functional tracking system based on triboelectric-electromagnetic hybridized blue energy harvesting module, Nano Energy 72 (2020) 104684.
[93] H. Yang, M. Deng, Q. Tang, W. He, C. Hu, Y. Xi, R. Liu, Z.L. Wang, A nonencapsulative pendulum-like paper–based hybrid nanogenerator for energy harvesting, Adv. Energy Mater. 9 (2019) 1901149.
[94] J. Wang, L. Pan, H. Guo, B. Zhang, R. Zhang, Z. Wu, C. Wu, L. Yang, R. Liao, Z. L. Wang, Rational structure optimized hybrid nanogenerator for highly efficient water wave energy harvesting, Adv. Energy Mater. 9 (2019) 1802892.
[95] Y. Bai, L. Xu, C. He, L. Zhu, X. Yang, T. Jiang, J. Nie, W. Zhong, Z.L. Wang, High-performance triboelectric nanogenerators for self-powered, in-situ and real-time water quality mapping, Nano Energy 66 (2019) 104117.
[96] H. Yang, M. Wang, M. Deng, H. Guo, W. Zhang, H. Yang, Y. Xi, X. Li, C. Hu, Z. Wang, A full-packaged rolling triboelectric-electromagnetic hybrid nanogenerator for energy harvesting and building up self-powered wireless systems, Nano Energy 56 (2019) 300–306.
[97] Y. Chen, Y. Cheng, Y. Jie, X. Cao, N. Wang, Z.L. Wang, Energy harvesting and wireless power transmission by a hybridized electromagnetic–triboelectric nanogenerator, Energy Environ. Sci. 12 (2019) 2678–2684.
[98] W. Wang, J. Xu, H. Zheng, F. Chen, K. Jenkins, Y. Wu, H. Wang, W. Zhang, R. Yang, A spring-assisted hybrid triboelectric–electromagnetic nanogenerator for harvesting low-frequency vibration energy and creating a self-powered security system, Nanoscale 10 (2018) 14747–14754.
[99] Y. Wu, Q. Zeng, Q. Tang, W. Liu, G. Liu, Y. Zhang, J. Wu, C. Hu, X. Wang, A teeterboard-like hybrid nanogenerator for efficient harvesting of low-frequency ocean wave energy, Nano Energy 67 (2020) 104205.
[100] X. Chen, L. Gao, J. Chen, S. Lu, H. Zhou, T. Wang, A. Wang, Z. Zhang, S. Guo, X. Mu, Z.L. Wang, Y. Yang, A chaotic pendulum triboelectric-electromagnetic hybridized nanogenerator for wave energy scavenging and self-powered wireless sensing system, Nano Energy 69 (2020) 104440.
[101] Z. Wu, H. Guo, W. Ding, Y.-C. Wang, L. Zhang, Z.L. Wang, A hybridized triboelectric–electromagnetic water wave energy harvester based on a magnetic sphere, ACS Nano 13 (2019) 2349–2356.
[102] X. Wang, Z. Wen, H. Guo, C. Wu, X. He, L. Lin, X. Cao, Z.L. Wang, Fully packaged blue energy harvester by hybridizing a rolling triboelectric nanogenerator and an electromagnetic generator, ACS Nano 10 (2016) 11369–11376.
[103] C. Hao, J. He, C. Zhai, W. Jia, L. Song, J. Cho, X. Chou, C. Xue, Two-dimensional triboelectric-electromagnetic hybrid nanogenerator for wave energy harvesting, Nano Energy 58 (2019) 147–157.
[104] R. Cao, T. Zhou, B. Wang, Y. Yin, Z. Yuan, C. Li, Z.L. Wang, Rotating-sleeve triboelectric–electromagnetic hybrid nanogenerator for high efficiency of harvesting mechanical energy, ACS Nano 11 (2017) 8370–8378.
[105] Z.L. Wang, Entropy theory of distributed energy for internet of things, Nano Energy 58 (2019) 669–672.
[106] J.H. Wang, T.Y.Y. He, C. Lee, Development of neural interfaces and energy harvesters towards self-powered implantable systems for healthcare monitoring and rehabilitation purposes, Nano Energy 65 (2019).
[107] S. Lee, Q.F. Shi, C. Lee, From flexible electronics technology in the era of IoT and artificial intelligence toward future implanted body sensor networks, Apl. Mater. 7 (2019).
[108] Q.F. Shi, T.Y.Y. He, C. Lee, More than energy harvesting - combining triboelectric nanogenerator and flexible electronics technology for enabling novel micro-/nano-systems, Nano Energy 57 (2019) 851–871.
[109] A.A. Khan, A. Mahmud, D. Ban, Evolution from single to hybrid nanogenerator: a contemporary review on multimode energy harvesting for self-powered electronics, IEEE Trans. Nanotechnol. 18 (2019) 21–36.

Long Liu received his Ph.D. degree from Beijing Institute of Nano energy and Nanosystems, Chinese Academy of Sciences in 2018. He is currently a Research Fellow in the Department of Electrical and Computer Engineering, National University of Singapore. His research interests are focused on energy harvesters and self-powered sensors, wearable electronics, IoT applications in the 5G era.

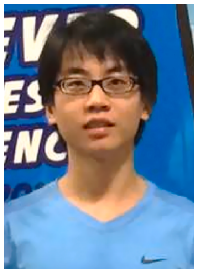

Qiongfeng Shi received his B.Eng. degree from the Department of Electronic Engineering and Information Science, University of Science and Technology of China (USTC) in 2012, and received his Ph.D. degree from the Department of Electrical and Computer Engineering, National University of Singapore (NUS) in 2018. He is currently a Research Fellow in the Department of Electrical and Computer Engineering, National University of Singapore. His research interests include energy harvesters, triboelectric nanogenerators, self-powered sensors, and wearable/implantable electronics.

Chengkuo Lee received his Ph.D. degree in Precision Engineering from The University of Tokyo in 1996. Currently, he is the director of Center for Intelligent Sensors and MEMS at National University of Singapore, Singapore. In 2001, he cofounded Asia Pacific Microsystems, Inc., where he was the Vice President. From 2006 to 2009, he was a Senior Member of the Technical Staff at the Institute of Microelectronics, A-STAR, Singapore. He has contributed to more than 330 peer-reviewed international journal articles. His ORCID is 0000- 0002-8886-3649.